J. Am. Chem. Soc. **1994,** *116,* 9203–9205

Nonlinear Optical Activity and Biomolecular Chirality

**Thierry Verbiest,[†] Martti Kauranen,[†] André Persoons,[*,†] Marjo Ikonen,[‡]
Jouni Kurkela,[§] and Helge Lemmetyinen[§]**

Contribution from the Laboratory of Chemical and Biological Dynamics, University of Leuven, B-3001 Heverlee, Belgium, Department of Physical Chemistry, University of Helsinki, P.O. Box 13, FIN-00014 Helsinki, Finland, and Institute of Materials Chemistry, Tampere University of Technology, P.O. Box 589, FIN-33101 Tampere, Finland

Received May 9, 1994[⊗]

Abstract: Circular-difference response of second-harmonic generation from chiral surfaces is shown to be a sensitive probe of chiral biological samples. The sensitivity of this nonlinear effect is several orders of magnitude higher than that of linear circular dichroism and is demonstrated using samples of bacteriorhodopsin. This nonlinear optical activity probes molecular chirality on a more general level than linear techniques. Surface specifity of the novel approach can be of considerable importance in the study of biological membranes. Hence, this process has the potential of becoming a new chiro-optical tool in the fields of analytical (bio)chemistry, surface chemistry, and cell biology.

Chiral molecules respond differently to light with opposite circular polarizations. This optical activity of chiral molecules gives rise to effects such as circular dichroism, optical rotation, and optical rotatory dispersion.[1] Circular dichroism is based on unequal amounts of absorption experienced by left- and right-hand circularly-polarized beams of light as they pass through a sample of chiral medium. The circular-difference effect is described quantitatively by the normalized difference $\Delta\epsilon/\epsilon = 2(\epsilon_{\text{left}} - \epsilon_{\text{right}})/(\epsilon_{\text{left}} + \epsilon_{\text{right}})$ of the molar extinction coefficients for the two circularly-polarized components of light. Each chiral molecule exists in two different enantiomers that are mirror images of each other. For the two enantiomers, the results of circular-dichroism measurements are equal in magnitude but opposite in sign. This property makes circular dichroism a powerful tool to detect molecular chirality and to distinguish the two enantiomers from each other.[2] Due to the importance of chirality to living matter, the distinction between the two enantiomers is particularly important in biological and life sciences.[3] For several cases of chiral molecules, one enantiomer is extremely important for the life processes while the other enantiomer is unimportant or can be even harmful. For the case of pharmaceutical molecules, one enantiomer can have beneficial effects in the treatment of diseases while the other enantiomer can have severe counterproductive effects.[4]

Traditional optical-activity effects are linear optical effects; i.e., they result from the linear response of the molecular medium to the electromagnetic field. The fundamental basis of these effects lies in the structure of chiral molecules. As the electrons of chiral molecules are displaced from their equilibrium by the application of the electromagnetic field, they are forced to move along paths that are helical. This helical movement gives rise to an induced magnetic dipole moment of the molecule in addition to the usual electric dipole moment. For the same reason, chiral molecules also respond to the electric and magnetic components of the field. In quantum-mechanical terms, both electric and magnetic dipole transitions between the states of chiral molecules are important in determining their optical properties.[5]

Circular-difference effects have been predicted to occur also in nonlinear optical processes.[6–8] Such nonlinear optical activity was recently observed in second-harmonic generation from chiral molecules adsorbed at an air/water interface.[9] Second-harmonic generation is a surface-specific nonlinear optical process, and hence the possibility of a novel nonlinear surface circular-dichroism spectroscopy was proposed. We have found that second-harmonic generation from a chiral surface that consists of a Langmuir–Blodgett-deposited monolayer of synthetic chiral polymers has a different response to fundamental beams that are left- and right-hand circularly polarized.[10] To account for the effects of molecular chirality on the nonlinear response of the monolayer, we developed a model that includes the contributions of both electric and magnetic dipole transitions to the second-order nonlinearity.[11] This model was found to provide a good explanation of the observed circular-difference effects. In this paper, we show that this novel nonlinear effect can be observed in biological samples and that it could have a considerable impact in fields such as analytical (bio)chemistry, surface chemistry, and cell biology.

We demonstrate the strength of nonlinear optical activity as a probe of the chiral environment of biological samples by studying circular-difference effects in second-harmonic generation from bacteriorhodopsin.[12] Bacteriorhodopsin is the light-energy-transducing protein that is present in the purple membrane of halophilic bacteria. In the purple membrane, the protein is arranged into clusters of three that show stronger optical activity than individual protein molecules.[13] The trimers are arranged in a two-dimensional hexagonal lattice with $p3$ symmetry that extends across the size (up to 1 μm) of the purple membrane fragments.[14] Linear circular-dichroism spectra of suspensions of purple membrane in water typically show a relative circular-difference effect of $\Delta\epsilon/\epsilon = 0.1\%$.[13]

Our experimental setup is shown in Figure 1. The bacteriorhodopsin sample is illuminated with the intense (~100 MW/

---

[*] To whom the correspondence should be addressed.

[†] University of Leuven.

[‡] University of Helsinki.

[§] Tampere University of Technology.

[⊗] Abstract published in *Advance ACS Abstracts*, September 1, 1994.

(1) Applequist, J. *Am. Sci.* **1987**, *75*, 59.

(2) Mason, S. F. *Molecular Optical Activity and the Chiral Discriminations*; University Press: Cambridge, 1982.

(3) Cantor, C. R.; Schimmel, P. R. *Biophysical Chemistry Part II: Techniques for the Study of Biological Structure and Function*; W. H. Freeman & Company: San Francisco, 1980.

(4) Tomaszewski, J.; Rumore, M. M. *Drug. Dev. Ind. Pharm.* **1994**, *20*(2), 119.

(5) Condon, E. U. *Rev. Mod. Phys.* **1937**, *9*, 432.

(6) Andrews, D. L.; Thirunamachandran, T. *J. Chem. Phys.* **1979**, *70*, 1027.

(7) Lam, Y. T.; Thirunamachandran, T. *J. Chem. Phys.* **1982**, *77*, 3810.

(8) Wagnière, G. *J. Chem. Phys.* **1982**, *77*, 2786.

(9) Petralli-Mallow, T.; Wong, T. M.; Byers, J. D.; Lee, H. I.; Hicks, J. M. *J. Phys. Chem.* **1993**, *97*, 1383.

(10) Kauranen, M.; Verbiest, T.; Meijer, E. W.; Havinga, E. E.; Teerenstra, M. N.; Schouten, A. J.; Nolte, R. J. M.; Persoons, A. *Phys. Rev. Lett.*, submitted.

(11) Kauranen, M.; Verbiest, T.; Maki, J. J.; Persoons, A. *J. Chem. Phys.*, accepted for publication.

(12) Stoeckenius, W.; Bogomolni, R. A. *Annu. Rev. Biochem.* **1982**, *52*, 587.

(13) Becher, B.; Cassim, J. Y. *Biophys. J.* **1976**, *16*, 1183.

(14) Henderson, R. *J. Mol. Biol.* **1975**, *93*, 123.

0002-7863/94/1516-9203$04.50/0 © 1994 American Chemical Society

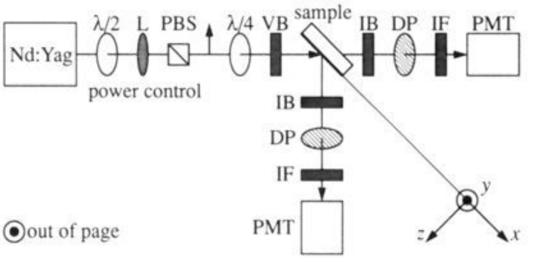

Figure 1. Schematic representation of the experiment. The fundamental beam of a Nd:YAG laser (1064 nm) is p polarized with respect to the sample (x–y plane) using a polarizing beam splitter (PBS). A half-wave ($\lambda/2$) plate is used to control the power of the laser. A quarter-wave ($\lambda/4$) plate is used to convert the polarization from linear to right-hand or left-hand circular. The beam is focused by a 200-mm focal length lens (L) onto the sample. The flash lamps of the laser are isolated from the experiment by a visible-blocking filter (VB). The reflected and transmitted second-harmonic beams are passed through an infrared blocking filter (IB) and a 532-nm interference filter (IF) before detection by photomultipliers (PMT). Dichroic sheet polarizers (DP) are used to analyze the distribution of second-harmonic radiation in s and p polarizations. In the actual experiments, only one detection channel was used either in the reflected or in the transmitted direction although both possible situations are shown in the figure.

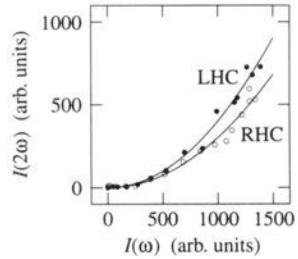

Figure 2. Quadratic dependence $I(2\omega) = QI^2(\omega)$ of the intensity of the second-harmonic field on that of the fundamental beam for left- (LHC, solid circles) and right-hand (RHC, open circles) circularly-polarized fundamental beams. The solid lines represent quadratic fits to the experimental data points. The sample used was bacteriorhodopsin embedded in a 2.5–4.8-nm thick film of soya phosphatidylcholine, the laser used was a 200-ps mode-locked Nd:YAG laser, and the transmitted p-polarized signal was detected.

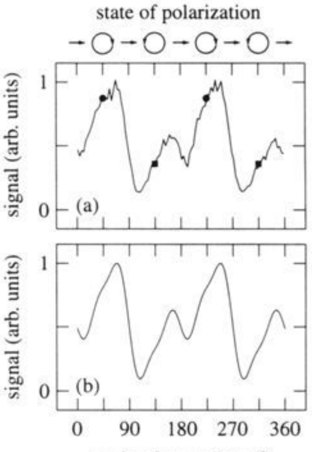

Figure 3. Experimental (a) and theoretical (b) results for the intensity of the s-polarized component of the second-harmonic field that is generated in the transmitted direction from fragments of purple membrane containing bacteriorhodopsin. The laser used was an injection seeded Nd:YAG laser with a ~10-ns pulse length. The plots are shown as functions of the rotation angle of the quarter-wave plate that was used to control the state of polarization of the fundamental beam. The linear polarization corresponds to a p-polarized fundamental field with respect to the sample. The intensities of the second-harmonic field for the two opposite circular polarizations of the fundamental field are indicated by the circles and the squares.

cm^2) beam of a mode-locked (1064 nm, ~200-ps pulse length, 10-Hz repetition rate) or an injection seeded (1064 nm, ~10-ns pulse length, 10-Hz repetition rate) Nd:YAG laser. The polarization of the incident beam is varied from linear to left- and right-hand circular by means of a quarter-wave plate. The angle of incidence is ~45°, and the intensity of the generated s- and p-polarized second-harmonic light at 532 nm is recorded in reflection or in transmission. For practical reasons, most measurements were made on the transmitted signals.

We first used the mode-locked Nd:YAG laser to investigate bacteriorhodopsin molecules that are embedded in a Langmuir–Blodgett film.[15] In the films, the bacteriorhodopsin molecules were in a soya phosphatidylcholine matrix in a molar ratio of 1:28. The thickness of the film, determined by a scanning tunneling microscope,[16] varied from 5.0 to 9.6 nm. In such a film, the bacteriorhodopsin molecules can exhibit local ordering in a lattice similar to the one that occurs in purple membrane.[16] In spite of this local ordering, the molecules are randomly distributed on a scale that is much smaller than an optical wavelength. Hence, the film constitutes an isotropic surface with full rotational symmetry about the surface normal. The intensity of the second-harmonic light scales as the square of the intensity of the fundamental light:

$$I(2\omega) = QI^2(\omega) \tag{1}$$

We have determined the quadratic coefficients Q for the bacteriorhodopsin films using left- and right-hand circularly-polarized fundamental beams. The results are shown in Figure 2 for the p-polarized transmitted component of the second-harmonic field and show clearly that the efficiency of second-harmonic generation depends on the helicity of the fundamental beam. Analogous to linear circular dichroism, we express this circular-difference effect in terms of the sum and difference of the intensities (or, equivalently, of the quadratic coefficients) of the detected second-harmonic light for left- and right-hand circularly-polarized excitation as $\Delta I/I = 2(I_{\text{left}} - I_{\text{right}})/(I_{\text{left}} + I_{\text{right}})$. For the results of Figure 2, this circular-difference effect is about 25%. For the s-polarized transmitted signal, the circular difference is about 13%.

While the use of bacteriorhodopsin Langmuir–Blodgett films has the advantage of providing a well-characterized sample, they are, however, not convenient in potential applications of the present effect as a routine probe of biomolecular chirality. To assess the usefulness of the effect for other, more practical, types of samples, we have placed a drop of purple membrane suspension in water between two glass slides. Such a sample preparation technique typically results in a sample thickness of the order of 1 μm, which was verified by a spectrophotometer measurement. This technique results in samples for which the overall efficiency of second-harmonic generation depends on the spot on the sample that is illuminated by the laser. This inhomogeneity is most likely an indication of aggregation of the purple-membrane fragments. Nevertheless, these samples also exhibit a strong circular-difference response, which for the s-polarized transmitted signal is ~100% as shown in Figure 3(a). These results are obtained by continuously rotating the quarter-wave plate to vary the polarization of the fundamental beam from left-hand circular to linear to right-hand circular. The p-polarized transmitted and the two reflected signals also exhibit a circular-difference response, which varies from ~5% to ~60% depending on the signal.

For a theoretical explanation of our experimental results, we include the contributions of electric and magnetic dipole transitions to the second-order nonlinearity of the chiral surface. In this model, the electric polarization at the second-harmonic frequency

---

[15] Ikonen, M.; Peltonen, J.; Vuorimaa, E.; Lemmetyinen, H. *Thin Solid Films* **1992**, *213*, 277.

[16] Niemi, H. E.-M.; Ikonen, M.; Levlin, J. M.; Lemmetyinen, H. *Langmuir* **1993**, *9*, 2436.

is taken to be of the form

$$P_i(2\omega) = \sum_{j,k} [\chi^{\mathrm{eee}}_{ijk} E_j(\omega)\, E_k(\omega) + \chi^{\mathrm{eem}}_{ijk} E_j(\omega)\, B_k(\omega)] \quad (2)$$

Similarly, the magnetization at the second-harmonic frequency is of the form

$$M_i(2\omega) = \sum_{j,k} \chi^{\mathrm{mee}}_{ijk} E_j(\omega)\, E_k(\omega) \quad (3)$$

In eqs 2 and 3, $\mathbf{E}(\omega)$ and $\mathbf{B}(\omega)$ are the electric field and the magnetic induction field at the fundamental frequency, respectively. The subscripts i, j, and k refer to Cartesian coordinates, and the superscripts e and m refer to electric and magnetic dipole interactions between the molecules and the light field, respectively. Thus, $\chi^{\mathrm{eee}}_{ijk}$ is the usual second-order nonlinear susceptibility, which depends only on electric dipole transitions, and $\chi^{\mathrm{eem}}_{ijk}$ and $\chi^{\mathrm{mee}}_{ijk}$ are susceptibilities that account for the contributions of magnetic dipole transitions to the nonlinearity.[17,18] The magnetic dipole interaction is treated only to first order because, even in chiral molecules, it is weaker than the electric dipole interaction. The nonlinear polarization and magnetization act as sources for the second-harmonic field. The intensity of the second-harmonic field as a function of the state of polarization of the fundamental beam can be directly calculated from eqs 2 and 3 and from the radiative properties of electric and magnetic dipoles. The second-harmonic field is found to be

$$\mathbf{E}(2\omega) \sim [\mathbf{n} \times \mathbf{P}(2\omega)] \times \mathbf{n} - \mathbf{n} \times \mathbf{M}(2\omega) \quad (4)$$

where $\mathbf{n}$ is the direction of observation.

The number of nonvanishing and independent components of tensors χ^{eee}, χ^{eem}, and χ^{mee} is limited by the symmetry of the surface. For an isotropic distribution of chiral molecules in the plane of the surface (assumed to be x–y plane, see Figure 1), the independent components of χ^{eee} are zzz, zxx, xxz, and xzy, of which xzy is allowed only by chirality; those of χ^{mee} are zzz, zxx, xxz, and xzy, of which zzz, zxx, and xxz are allowed only by chirality; and those of tensor χ^{eem} are zzz, zxx, xxz, xzx, zxy, xyz, and xzy, of which zzz, zxx, xxz, and xzx are allowed only by chirality.[11] It can be shown that the intensities of all second-harmonic fields can be expressed in terms of only three different functions of the rotation angle of the wave plate.[11] The expansion coefficients of these three functions depend on the independent components of the three tensors and are different for each second-harmonic signal.

A theoretical fit to the experimental results of Figure 3a based on this model under the assumption of an isotropic surface is shown in Figure 3b. The fit has been obtained under the assumption, which is strictly valid only under nonresonant excitation, that the components of the electric-dipole-allowed susceptibility tensor χ^{eee} are real quantities and those of tensors χ^{eem} and χ^{mee} are imaginary quantities.[17] The circular-difference response arises from the interference between these real and imaginary contributions to the nonlinearity. The fit yields the relative values for the following combinations of components of the three tensors:

$$\chi^{\mathrm{eee}}_{xxz} = 0.35$$

$$-(\chi^{\mathrm{eem}}_{xzy} + \chi^{\mathrm{eem}}_{xyz}) \cos\theta + 2\chi^{\mathrm{mee}}_{xyz} \cos\theta = 1.5\mathrm{i}$$

$$-\chi^{\mathrm{eem}}_{xzx} + \chi^{\mathrm{mee}}_{zzz} \sin^2\theta + \chi^{\mathrm{mee}}_{\mathrm{zxx}} \cos^2\theta + 2\chi^{\mathrm{mee}}_{xxz} \cos^2\theta = \mathrm{i}$$

$$\chi^{\mathrm{eem}}_{xxz} + \chi^{\mathrm{mee}}_{zxx} = -0.4\mathrm{i} \quad (5)$$

where θ is the angle of incidence. It is important to note that the full interpretation of the results of Figure 3a is potentially more complicated than presented here. These complications arise from the fact that the individual purple membrane fragments have lower than isotropic symmetry that extends up to a scale of the order of an optical wavelength. Hence, the number of allowed components of the various susceptibility tensors for purple membrane fragments is larger than that for an isotropic surface. However, we presently believe that the very strong circular-difference response (~100%) that is evident in Figure 3a is due to the supramolecular chirality of bacteriorhodopsin trimers although further investigations are necessary for the complete description of these results.

Determination of molecular chirality by nonlinear optical activity has several advantages compared to linear circular-dichroism spectroscopy. In the present experiments, the value of the circular-difference effect $\Delta I/I$ is up to 3 orders of magnitude higher than that obtained by linear circular-dichroism spectroscopy from samples of bacteriorhodopsin.[13] Another advantage of the new effect is the small amount of material that is needed. In our experiments, we typically interacted with an amount of 10^{-13}–10^{-11} mol of bacteriorhodopsin. In order to perform a linear circular-dichroism experiment, approximately 10^{-8} mol of bacteriorhodopsin is typically needed.[13] Hence, the new nonlinear effect makes it possible to detect circular-difference effects with a higher accuracy from up to 5 orders of magnitude less material than linear circular-dichroism spectroscopy. We believe that the amount of material needed can easily be reduced by a further 2 orders of magnitude. Therefore it is evident that this technique can have important applications in analytical chemistry as well as in biological and pharmaceutical sciences to detect chirality from small amounts of molecules.

Further advantages of nonlinear optical activity are related to properties of second-harmonic generation. Linear optical-activity effects in isotropic solution are only sensitive to a certain combination of the components of electric and magnetic dipole transition moments between the ground state and the excited states of the molecules.[5] Hence, structural chirality of a molecule does not necessarily give rise to strong linear optical activity. Nonlinear optical activity, on the other hand, depends also on transition moments between different excited states. Furthermore, a large number of components of transition moments contribute to the second-order susceptibilities that are allowed by the symmetry of chiral surfaces. Hence, nonlinear optical activity can be used to probe molecular properties linked to chirality on a more fundamental level than the linear techniques. Chiral molecules with low linear optical activity could therefore give rise to an easily measurable nonlinear optical activity. A particularly intriguing feature of nonlinear optical activity is its sensitivity to chirality of simple nonlinear molecules[9] as well as to that of polymers in which the nonlinearity is localized, to the lowest order approximation, to achiral chromophores and chirality arises from the helical structure in the backbone.[10,11] These latter results suggest that the effect could also be utilized to address secondary structure of proteins. Another feature of nonlinear optical activity is its surface specificity, which arises from the symmetry properties of second-harmonic generation provided that the media on the two sides of the surface are isotropic.[19] This feature is important in surface chemistry and cell biology because the nonlinear approach makes the chiral environment of biological membranes and interfaces accessible to measurement.

Acknowledgment. We gratefully acknowledge discussions of this work with Y. Engelborghs. This research has been supported by the Belgian Government (IUAP-16) and by the Belgian National Science Foundation (FKFO 9.0012.92). M. K. is a research fellow of the University of Leuven.

---

(17) Pershan, P. S. *Phys. Rev.* **1963**, *130*, 919.

(18) Meijer, E. W.; Havinga, E. E.; Rikken, G. L. J. A. *Phys. Rev. Lett.* **1990**, *65*, 37.

(19) Shen, Y. R. *The Principles of Nonlinear Optics*; Wiley: New York, 1984.